Tellus
SERIES B
CHEMICAL
AND PHYSICAL
METEOROLOGY
PUBLISHED BY THE INTERNATIONAL METEOROLOGICAL INSTITUTE IN STOCKHOLM

Tellus (2009), 61B, 642–656
Printed in Singapore. All rights reserved

TELLUS

The effects of black carbon and sulphate aerosols in China regions on East Asia monsoons

By YU LIU[1]*, JIAREN SUN[2] and BAI YANG[3], [1]*Chinese Academy of Meteorological Sciences, 46 Zhongguancun South Street, Beijing 100081, P R China;* [2]*South China Institute of Environmental Sciences, Ministry of Environmental Protection, Guangzhou 510655, P R China;* [3]*Environmental Sciences Division, Oak Ridge National Laboratory, Oak Ridge, TN 37831, USA*

(Manuscript received 19 July 2008; in final form 9 April 2009)

ABSTRACT

In this paper, we examine the direct effects of sulphate and black carbon (BC) aerosols in China on East Asia monsoons and its precipitation processes by using the Community Atmosphere Model (CAM) 3.0 model. It is demonstrated that sulphate and BC aerosols in China both have the effects to weaken East Asia monsoons in both summer and winter seasons. However, they certainly differ from each other in affecting vertical structures of temperature and atmospheric circulations. Their differences are expected because of their distinct optical properties, that is, scattering versus absorbing. Even for a single type of aerosol, its effects on temperature structures and atmospheric circulations are largely season-dependent. Applications of *T*-test on our results indicate that forcing from BC aerosols over China is relatively weak and limited. It is also evident from our results that the effects of synthetic aerosols (sulphate and BC together) on monsoons are not simply a linear summation between these two types of aerosols. Instead, they are determined by their integrated optical properties. Synthetic aerosols to a large degree resemble effects of sulphate aerosols. This implies a likely scattering property for the integration of BC and sulphate aerosols in China.

1. Introduction

Sulphate and black carbon (BC), primarily originated from anthropogenic sources, are two of the most important radiatively active aerosols in the atmosphere. Previous studies showed that sulphate and BC aerosols tend to play opposite roles in their radiative effects. While the former is characteristic of strong radiation scattering and thus leads to a cooling surface (negative radiative forcing), the latter heats up the atmosphere owing to its excellent ability of absorbing solar radiation. On a global scale, the direct radiative forcing from sulphate aerosols is believed to range from -0.2 to -0.6 W m^{-2}; in contrast, it is approximately between 0.05 and 0.35 W m^{-2} from fossil fuel BC (IPCC, 2007).

A large number of studies have been conducted on the direct effects of sulphate and BC on climate system (Bolin and Charlson, 1976; Hansen et al., 1997; Luo et al., 1999, 2000, 2001; Jacobson, 2001; Ramanathan et al., 2001; Menon et al., 2002; Chen et al., 2004; Gu et al., 2006). By introducing an aerosol optical depth (AOD; measured at 0.75 μm) into the China Regional Climate Model (CRCM; Gong and Li, 1996), Luo et al. (1999) examined the climatic responses to the forcing of all aerosols including sulphate and BC. Their results showed that the region of the largest radiative forcing was in the Sichuan Basin and the second largest one at the Tibetan Plateau and Hetao area. Moreover, Chen et al. (2004) found that these AOD effects could well explain the cooling trend observed in the areas of Sichuan Basin and mid-Yangtze River between 1960 and 1980. A recent study by Jacobson and Kaufman (2006) further suggested a link between an increasing level of aerosols in the atmosphere over China continent and weaken wind in the same region. Absorbing aerosols (such as BC) emitted in the regions of East and South Asia were also believed to be responsible for precipitation anomalies, for example the 'wet south versus dry north' phenomenon in China in the last decade (Menon et al., 2002). However, this conclusion is not completely supported by Gu et al. (2006) who revealed that such a precipitation distribution was an integrated result from all aerosols with sulphate as a dominant factor over the absorbing aerosols (BC and others). In addition to precipitation, Gu et al. (2006) also analysed the aerosol effects on surface soil temperature, barometric pressure and cloud structures. Unfortunately, all above-mentioned conclusions were drawn on the assumption of uniformity of single-scattering albedo, despite its remarkable variations in both time and space that ultimately are rooted in the spatial and temporal variations of aerosols.

*Corresponding author.
e-mail: liuyu@cams.cma.gov.cn or liuycams@sina.com.
DOI: 10.1111/j.1600-0889.2009.00427.x

In contrast to the tremendous efforts spent on their radaitive forcing on climatic mean temperature, precipitation, pressure, etc., little attention has been given to the aerosols' effects on monsoon. East Asia summer monsoon system consists of a tropical monsoon positioned in the South China Sea and West Pacific, and a subtropical monsoon located along the coast of China–Japan. China is subject to strong influence of East Asia summer monsoon. Therefore, its climate is particularly affected by the interannual variation of monsoon position and intensity, especially in the flood season (May–September) when the variations of precipitation intensities and rain band position over Eastern China are closely correlated with summer monsoon activities (Chen et al., 1991). In recent years scientists started to realize the importance of aerosols' radiative forcing on monsoons and the induced precipitation (Singh et al., 2005). Such examples can be seen in Lau and Kim (2006) and Lau et al. (2006). By analysing a combined set of data from both modelling and observation, they put forward the elevated heat pump (EHP) hypothesis postulating that monsoon-induced rainy season might start earlier in North India and Nepal regions in May–June under the conditions of increased dust particles and absorbing aerosols (BC and others) in India and its surrounding regions along with the geographical forcing of Tibetan Plateau. Consequently, summer precipitation (June–July) in East Asia and its neighbouring oceans could be suppressed because of the enhanced India Monsoon and the induced northern displacement of Meiyu. Although this study greatly emphasized the joint effects on summer monsoon precipitation in India from the Plateau and absorbing aerosols, their discussion on the effects of sulphate and BC in East China was very limited. In fact, very high values of AOD have been observed in East China and its radiative forcing effects on the vertical profiles of air temperature, barometric pressure and ultimately on East Asia monsoon must be profound.

Similarly, East Asia winter monsoons also play an important role in the regional climate. It has been reported that East Asia winter monsoons to some degrees regulate the amount and distribution of precipitation in Malaysia, Indonesia and Australia (Chen et al., 1991), as well as large-scale tropical convection and precipitation in West Pacific (Chang and Lau, 1982; Lau and Boyle, 1987). Extended influences of East Asia winter monsoon are reflected in the variation of sea surface temperature (Bueh and Ji, 1999), the intensities of the Mongolia High and Aleutian Low, the magnitudes of pressure perturbation between Europe–Asia continent and North Pacific, and strength of winter storms (Pei and Li, 2007). Given its striking importance, we will extensively investigate in this paper the effects of sulphate and BC on East Asia monsoon and precipitation in China. Our analyses will also be extended to the mechanisms of the aerosols effects.

2. Model or model description

In this paper we employed the Community Atmosphere Model (CAM) 3.0, which is the fifth generation of the NCAR atmospheric GCM, and the atmosphere model of Community Climate System Model (CCSM) 3.0 . Not only can CAM3.0 be operated independently on atmospheric processes, but it can also be coupled with other earth process modules such as ocean, sea ice and ecology. Moreover, CAM 3.0 itself contains a well-developed land surface module (Community Land Model 3.0 or CLM 3.0) and two simplified versions of ocean modules (SOM and DOM). CAM 3.0 offers three options on its dynamical core, spectral Eulerian dynamics, semi-Lagrange dynamics and finite-volume dynamics (FV), and four levels of resolutions (T85, T63, T42 and T31) are available in the spectral Eulerian dynamical core. In the model, σ–P coordination is adopted with 26 vertical levels. The top boundary of the model is at the level of 2.917 hPa if T42 resolution is chosen. The model also contains an off-line aerosol assimilation module.

The spectral Eulerian dynamical core with its T42 resolution was used in all of our experiments. Such a resolution is equivalent to $2.8^\circ \times 2.8^\circ$ in a horizontal grid meshwork. Meanwhile, the ocean module Data Ocean Model (DOM) was used to read in climatic monthly mean sea surface temperature (SST) from an input dataset. We also introduced into this model an aerosol assimilation system (Collins et al., 2001, 2002) that essentially assimilated aerosol data from Model for Atmospheric Chemistry and Transport 4 (MATCH4) (Rasch et al., 1997) with AOD data from NOAA Pathfinder II (Stowe et al., 1997) as an input dataset. Radiation scheme (δ-Eddington) was taken from Collins et al. (2004).

3. Data and model validation

3.1. Data

Included in the model are four types of aerosols, sulphate, dust, sea-salt and carbonaceous aerosols. The last one is composed of organic carbon (OC) and BC. Aerosols' data used in this model were assimilated from modelling results (MATCH) and NOAA Pathfinder II data. In MATCH, sulphate cycle was treated using the scheme from Barth et al. (2000) and Rasch et al. (2000) and the data of anthropogenic emission of SO_2 were taken from Smith et al. (2001). Sources of dust aerosols were determined in a same manner as Zender et al. (2003) and Mahowald et al. (2003), and an empirical formula from Blanchard and Woodcock (1980) was used to compute the vertical profiles of sea salt aerosol concentration (μg m^{-3}). For the three subsets of carbonaceous aerosols, data for biomass-burning aerosols were taken from Liousse et al. (1996), fossil fuel aerosols from Cooke et al. (1999) and naturally emitted OC aerosols from the emission of terpene. In all numerical experiments (described in next section) the background AOD was set at 0.2, the same value used by Gu et al. (2006). With all data above, we were able to estimate the monthly averaged mass path (kg m^{-2}) for each aerosol type at all atmospheric layers.

3.2. Model validation

To validate the aerosols' data, we compared the global distribution of simulated AOD from our model with an average one from MODIS for the years from 2002 to 2005. The results are shown in Figs. 1 (summer) and 2 (winter). In summer (Fig. 1), a close agreement between the simulated AOD and the MODIS-derived AOD is seen in many areas, including East China and Tibetan Plateau, India, Middle East, South America and North Africa. On the other hand, difference exists in some other regions. Compared to MODIS data, for example, the predicted AOD is slightly higher in Europe and high latitudes of the Northern Hemisphere but lower in Middle Africa. Another area of discrepancy is located at northwest China and Middle Asia with higher AOD from MODIS than from our model. The likely reason lies in the treatment of dust storm flux in the model that may not be well adjusted for this area. In winter (Fig. 2), the predicted AOD is in accord with the MODIS data in East China and Tibetan Plateau, South and Southeast Asia, and Africa. However, our model seems to overestimate AOD in the regions of South America, Australia, and high latitudes of the Southern Hemisphere. Overall, our model successfully reproduced the primary features of global distribution of aerosols with the best agreement achieved in the area of our interest (East China) for both seasons.

We further validated our model by comparing the predicted mean precipitation and surface temperature to the NCEP reanalysis data for the period of 1965–2005 (figures not shown). Global distribution of predicted mean precipitation is largely in harmony with that of NECP reanalysis data. Both datasets show a maximum zone of mean precipitation in the tropical regions and zones of relatively large values at the middle latitudes of the Southern Hemisphere as well as in North Pacific and North Atlantic. However, it appears that our model overestimates the daily mean precipitation along the equator but underestimates it in South China. An overall agreement was also achieved on surface temperature between our predicted values and NECP reanalysis data, except that our model slightly over-predicted in the tropical regions. Based on all above comparisons we conclude that our model is capable of reproducing the main climatic characteristics on a global scale, which lends us confidence in employing it in the present study.

3.3. Experiments

Four numerical experiments were conducted for the investigation of climatic responses to the anthropogenic aerosols in China. One of them was a control experiment (Aeroworld) while the other three were sensitivity ones (Sulphate0, BC0 and China0). In Aeroworld five types of aerosols, sulphate, dusts, sea salt, OC and BC, were included in the global domain and these data were taken from MATCH. In each of the sensitivity experiments, one or some types of aerosols were eliminated in the areas of China while all others retained. As such, no sulphate aerosol was included in Sulphate0; no BC aerosol in BC0; and neither sulphate

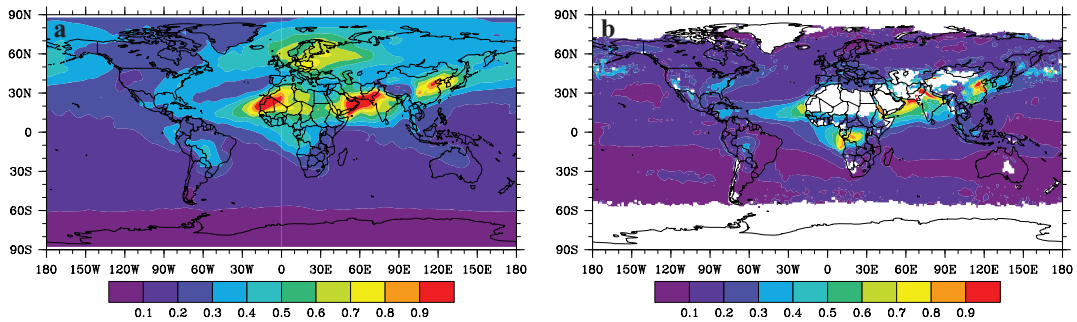

Fig. 1. AOD distribution in summer: (a) CAM 3.0 model data and (b) MODIS data averaged from 2002 to 2005.

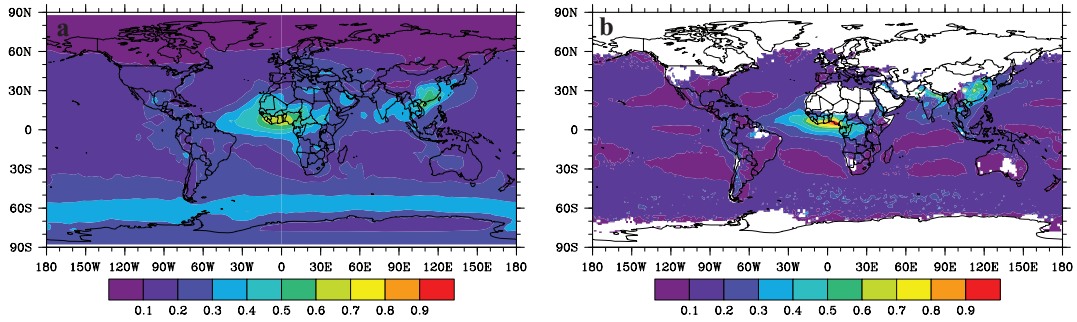

Fig. 2. AOD distribution in winter: (a) CAM 3.0 model data and (b) MODIS data averaged from 2002 to 2005.

nor BC in China0. In all experiments, the model was integrated for a period of 55 yr. Considering the first 15 yr of simulation time as the model spin-up stage, data during this period were excluded in our analyses. *T*-tests were carried out to detect the significant features in model outputs.

3.4. Definition of monsoon index

Typically monsoon strength is closely related with its area and intensity in the region of 20°N–40°N, 100°E–140°E. Following Qiao et al. (2002), we defined monsoon indices by considering monsoon area and intensity separately.

Area index (Asw) and intensity index (Isw) for southwest monsoon ($u > 0$, $v > 0$):

$$\mathrm{Asw} = \mathrm{Nsw/N}, \quad \mathrm{Isw} = \sum \mathrm{Usw/Nsw};$$

Area index (Ase) and intensity index (Ise) for southeast monsoon ($u < 0$, $v > 0$):

$$\mathrm{Ase} = \mathrm{Nse/N}, \quad \mathrm{Ise} = \sum \mathrm{Use/Nse};$$

Area index (An) and intensity index (In) for north monsoon ($v < 0$):

$$\mathrm{An} = \mathrm{Nn/N}, \quad \mathrm{In} = \sum \mathrm{Un/Nn},$$

where Usw is the wind speed at a grid point at which southwest wind occurs and Nsw denotes the total number of such grid points, Use and Nse for southeast wind, and Un and Nn for north wind. N indicates the total number of grid points in the simulation domain.

4. Aerosols' effects on summer (JJA) monsoon

4.1. Sulphate aerosol

Figure 3 shows the spatial distribution of column density of sulphate aerosol in China with data extracted from the lowest vertical level of the model. It is evident that a centre of high column density is located in the Sichuan Basin with a peak value as high as 12 mg m^{-2} in summer. A second zone of high column density takes a southwest–northeast orientation covering the areas of south, middle, north and northeast China. Its centre is over North China with a maximum value of 6 mg m^{-2}. Other localized centres of high values can be seen in northwest China, such as over Xinjiang.

The model results show that sulphate aerosols in the China regions yield a radiative forcing of -0.25 W m^{-2} on the global scale. In response to this negative forcing, global averages of surface temperature, surface pressure and precipitation all drop off and the decreasing amounts are about 0.02 °C, 0.25 Pa and 0.16 mm d^{-1}, respectively. Given its geographical location, it is not surprising that the influence of sulphate aerosol in China to surface temperature is mainly confined to the Northern Hemisphere. The induced changes of surface temperature and pressure by sulphate aerosols in China areas are shown in Fig. 4. In Fig. 4a, a decrease of surface temperature is seen almost everywhere to the north of 25°N. Corresponding to sulphate aerosol distribution, three areas of the strongest cooling are located at the Sichuan Basin, northwest and northeast China with a magnitude of -0.7 °C or so. Our results agree on the locations of sulphate-induced cooling in July reported by Tian et al. (2005), but overestimate the cooling by 0.3–0.4 °C. Another similar study, that also examined the sulphate-induced cooling in July, reported agreeable results to ours in northwest and northeast China (Gu et al., 2006). However, Gu et al. failed to show a strong cooling area in the Sichuan Basin. They instead showed a temperature drop of -2 °C in Korea, Japan and the surrounding oceans. In term of the cooling magnitudes, our results are in the middle of Gu et al. and Tian et al. In addition, we believe the strong cooling in the Sichuan Basin is certainly reasonable because of the persistent high AOD values in this area (Luo et al., 1999). In contrast to the cooling to the north of 25°N, a temperature increase of 0.3–0.5 °C is observed in the areas to the south of this line, including South China and southeast coast area. Moreover this warming is further extended into the oceans. For example, air temperature above ocean increases by 0.3 °C in South China Sea. The temperature changes in most areas of China are

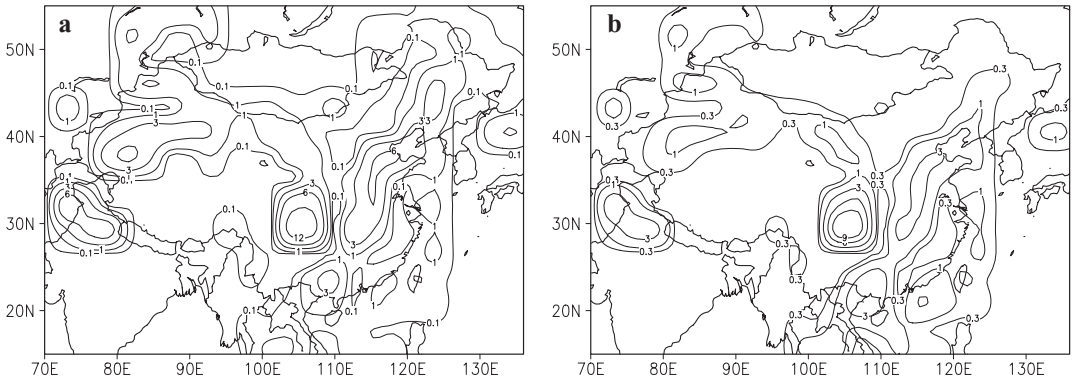

Fig. 3. Column density (mg m^{-2}) of sulphate aerosol at the lowest level of model: (a) in summer and (b) in winter.

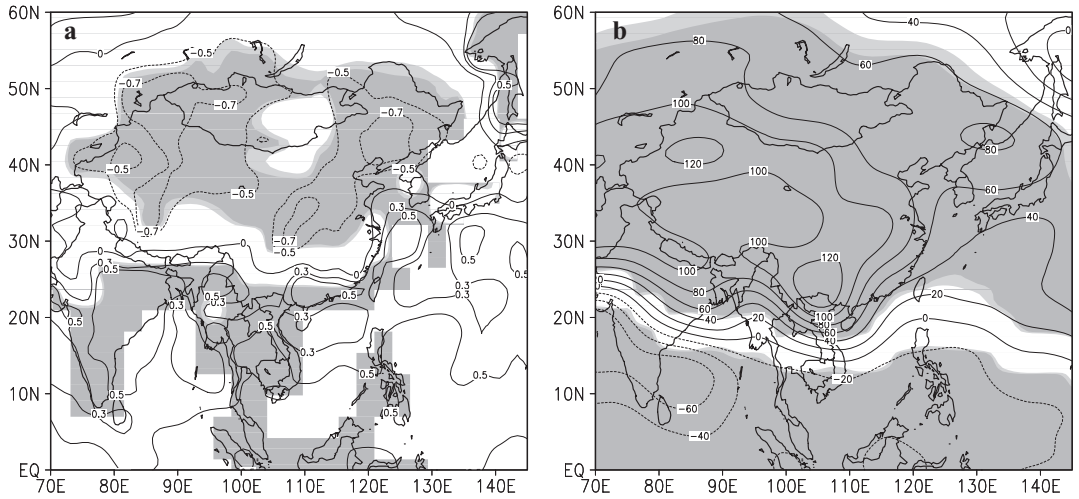

Fig. 4. Changes of: (a) surface temperature (K) and (b) surface pressure (Pa) in summer induced by sulphate aerosol. Dark and light shades indicate a confidence level of 95 and 90%, respectively, from the *T*-test.

significant at a 90% confidence level, whereas there is a much smaller area over the oceans where such a significant level of temperature increase can be found. The induced-changes in the fields of sensible heat flux, latent heat flux, water vapour and relative humidity (figures not shown) reveal that in most areas changes in surface temperature are closely linked to sensible heat and latent heat fluxes, while in some other areas heat transportation also plays a role. Over the ocean latent heat flux is the main factor in driving the temperature change. Sequential changes are observed to follow the aerosol's forcing, including air temperature, pressure, wind, water vapour, sensible heat and latent heat fluxes, and cloud. In most areas over the ocean, the increase of air temperature is a result of the increased water vapour in atmosphere and the enhanced latent heat flux. Changes in surface pressure (Fig. 4b) correspond very well to surface temperature. As a result of cooling in a large area over the land, surface pressure increases dramatically with a maximum increase of 120 Pa in the southwest China. Accompanied to this is a decrease of surface pressure over the oceans. Ultimately, summer monsoons that usually blow from ocean to land are expected to weaken because of the decreased pressure gradient between them.

East Asia summer monsoon is a typical and distinguished feature on summer 850 hPa weather map. Moisture air is carried into China through three distinct channels: (1) the first one passes through India and North India and wanders along the south side of Tibetan Plateau before it enters into China (southwest monsoon); (2) the second one starts from Indian Ocean and takes the route of the Bay of Bengal to South China Sea (tropical monsoon); (3) and the third one is along the south and southwest edges of the subtropical high in the Pacific (southeast monsoon or subtropical monsoon). The stretches of these monsoons become southerly wind over East China, veer east to the north of 35°N before they finally exit from northeast China. In

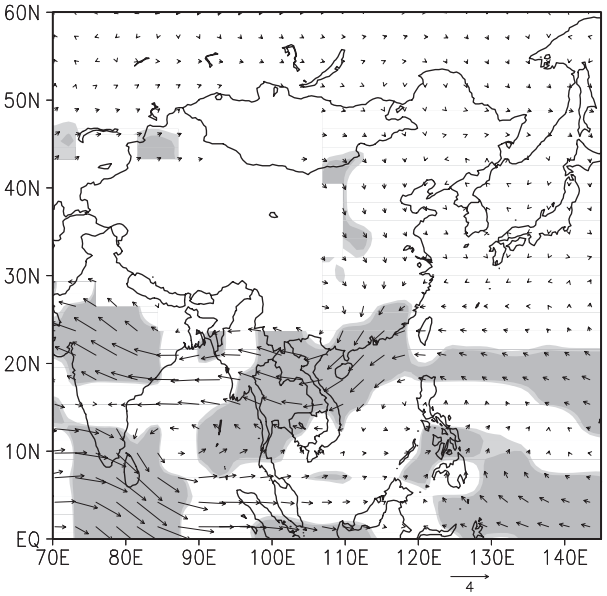

Fig. 5. Difference of horizontal wind (m s^{-1}) at 850 hPa in summer induced by sulphate aerosol. Dark and light shades indicate a confidence level of 95 and 90%, respectively, from the *T*-test.

Fig. 5, which shows the difference of mean wind field at 850 hPa between the Aeroworld and Sulphate0 experiments, an anticyclone forms around Tibetan Plateau and southwest China. The existence of this anticyclone must weaken both southwest and southeast monsoons, and the greatest weakening is predicted to occur in South China, Indochina Peninsula and central India. On the other hand, northerly wind strengthens to some degrees in the areas to the north of 35°N. In other words, the subtropical high in West Pacific shifts southeastward and wind associated with subtropical monsoon becomes weak over East China. All of

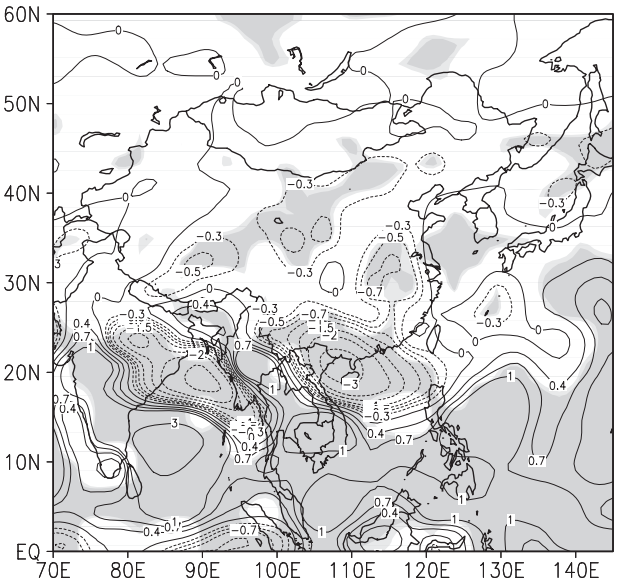

Fig. 6. Change of precipitation (mm d^{-1}) induced by sulphate aerosol in summer over China. Dark and light shades indicate a confidence level of 95 and 90%, respectively, from the *T*-test.

these results are consistent to those from Jacobson and Kaufman (2006).

Figure 6 shows the changes of precipitation in summer caused by sulphate aerosols. There are four regions showing relatively large amounts of precipitation reduction. Among them, the largest amount of reduction (-3 mm d^{-1}) is seen in the region between South China and South China Sea. An intermediate reduction of -0.7 mm d^{-1} is found at the middle and lower reaches of Yangtze River. Although precipitation reduction is predicted as little as about -0.3 mm d^{-1} at the Loess Plateau and Tibetan Plateau, this sulphate-induced change can be catastrophic to this region because its annual precipitation only ranges from 200 to 500 mm. Over the oceans, however, an opposite situation is observed, that is, precipitation increases in south and southeast parts of South China Sea and in West Pacific as well. Our results are clearly in contradiction with the findings from Gu et al. (2006) who suggested that sulphate aerosols could lead to an increased amount of precipitation in South China in July, although both studies agree on the change of precipitation in many areas outside of China including Arabian Sea, India Peninsula, Myanmar and south part of the Bay of Bengal. To further examine the sulphate-related precipitation changes, we present in Fig. 7 the changes of convective precipitation and large-scale precipitation. The changes of convective precipitation are in line with that of total precipitation (Fig. 6). This indicates that sulphate aerosols are an overwhelming factor in impacting convective precipitation, but a secondary one in affecting large-scale precipitation. In other words, sulphate-induced changes of total precipitation are to a large degree determined by the changes of convective precipitation.

Under normal conditions in summer, meridional circulation poses as a counter-clockwise rotation. As a result, northerly wind prevails at the level of 200 hPa while southerly wind dominates at the lower levels. Fig. 8 shows the sulphate-induced changes of meridional circulation and temperature averaged between 105°E and 120°E. Clearly negative radiative forcing resulted from sulphate aerosols lead to a sequence of dynamic and thermodynamic responses in the atmosphere. They are (1) cooling of air layers below 200 hPa to the north of 28°N, (2) development of subsidence motions between 15°N and 25°N, (3) enhancement of atmospheric stability and suppression of convective motions, (4) divergence at the lower levels of troposphere and (5) slowdown of northward transportation of moist

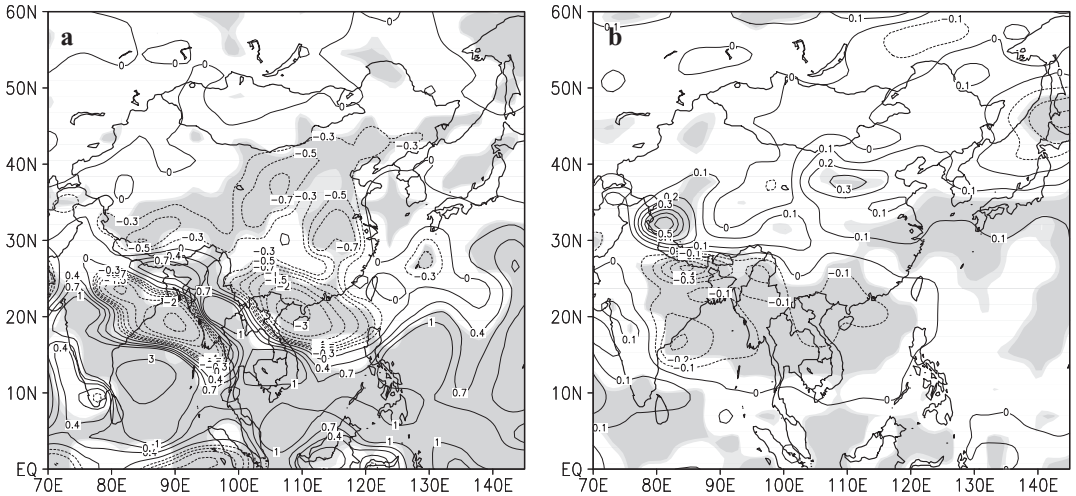

Fig. 7. Change of precipitation (mm d^{-1}) in summer: (a) convective precipitation and (b) large scale precipitation. Dark and light shades indicate a confidence level of 95 and 90%, respectively, from the *T*-test.

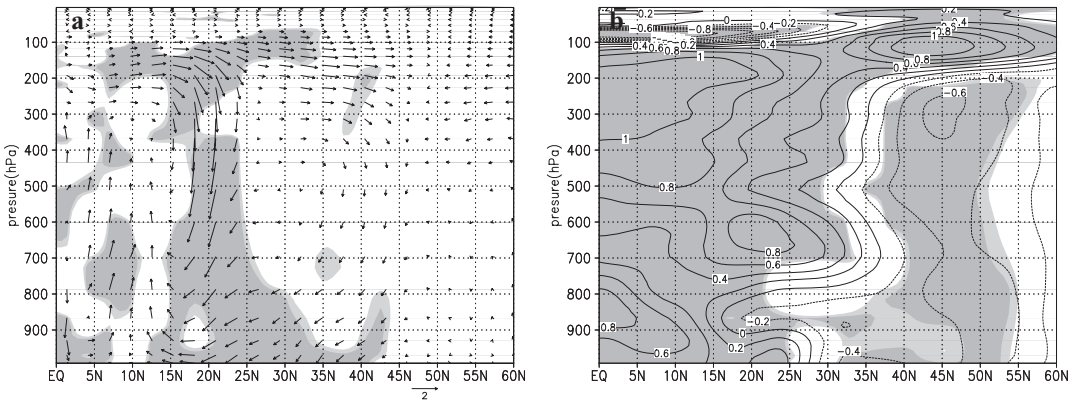

Fig. 8. Changes of: (a) the vertical meridional circulation and (b) temperature (K) zonally averaged between 105°E and 120°E in summer induced by sulphate aerosol. Dark and light shades indicate a confidence level of 95 and 90%, respectively, from the *T*-test.

air in the lower atmosphere. The consequence of these serial responses is the reduction of convective precipitation between 15°N and 25°N (Fig. 7a). Another feature in Fig. 8b is a cold tongue stretching southward at 850 hPa and between 20°N and 35°N, which further suppresses the upward motions and pushes the cold air southward. The mergence of cold air from north and warm air from south between 10°N and 15°N causes a strong upward motion that reaches upper levels of troposphere. At the level of 200–100 hPa, this upward motion starts to diverge and facilitates a clockwise circulation between 10°N and 25°N. Ultimately, the meridional circulation under normal climate condition weakens due to the offset of the induced clockwise circulation. This weakened meridional circulation may be responsible for the temperature increase to the south of 20°N.

In order to quantify the intensity changes of summer monsoons, we compared with the monsoon intensity indices (defined in Section 3.4) between Aeroworld and Surfate0 experiments. Given that East Asia summer monsoon is mainly driven by southwesterly and southeasterly winds, we applied this definition only to these two components. Our calculations suggested that intensity index in Sulphate0 case was reduced by 7.76% for southeast monsoon (Ise) and by 5.97% for southwest monsoon (Isw).

4.2. BC aerosol

BC aerosols spatial distribution in China greatly resembles that for sulphate aerosols. However, the former is in general one order smaller in magnitude than the latter in summer, and one fourth in winter. Again a centre of high column density is located in the Sichuan Basin with a peak value as high as 2.5 mg m^{-2} in winter. With a southwest–northeast orientation, the second zone of high column density covers the areas of south, middle, north and northeast China. Its centre is over North China with a maximum value of 1.4 mg m^{-2} in winter. The third region of high values sits in Xinjiang Province. Its value peaks at 0.2 mg m^{-2} in both summer and winter seasons (figure not shown).

The averaged results in the last 40 yr of our simulation indicate that the BC aerosols in China could result in a positive radiative forcing of 0.13 W m^{-2} on a global scale. On a global average pressure increases by 0.03 Pa while surface temperature and precipitation decrease by 0.02 °C and by an insignificant amount of 0.0048 mm d^{-1}, respectively. We illustrated in Fig. 9 the BC-induced variations of summer air temperature and precipitation in China. Notwithstanding a warming trend is observed in some areas such as Tibetan Plateau, South China and the central Xinjiang, the rest parts of China experiences a cooling trend (Fig. 9a). Among them, the strongest cooling about −0.5 to −0.4 °C takes place in the south part of northeast China and east part of Inner Mongolia; a small area with a cooling rate of −0.4 °C emerges along the border of Mongolia and the middle part of Inner Mongolia; another cooling area is located in Sichuan basin with a value of −0.3 °C or so. Overall, the total area influenced by the BC cooling effects is not as broad as that caused by sulphate aerosols. Other than the strong cooling centres, temperature changes anywhere else in China are insignificant at 90% confidence level. While precipitation increases in the middle and lower reaches of Yangtze River (Fig. 9b), it decreases in North and southwest China with a most significant decrease (about −0.5 mm d^{-1}; at 90% confidence level) in Sichuan Basin. Similar to sulphate aerosols, BC aerosols induce a serial of similar changes between the total precipitation and the convective precipitation. This can be explained by that BC aerosols are an overwhelming factor in convective precipitation.

Figure 10 shows the difference of wind field at 850 hPa between Aeroworld and BC0. Obviously effects of BC aerosols strengthen the southwest monsoon from the second channel, but at the same time weaken the south/southwest monsoon from the first channel and southeast monsoon from the third channel. The combination of these changes facilitates a formation of cyclonic circulation over the areas along and to the south of Yangtze River, which in turn results in a precipitation increase of 0.2 mm d^{-1} in the middle and lower reaches of Yangtze River (Fig. 9b). The additional effects from BC aerosols are that southerly wind over

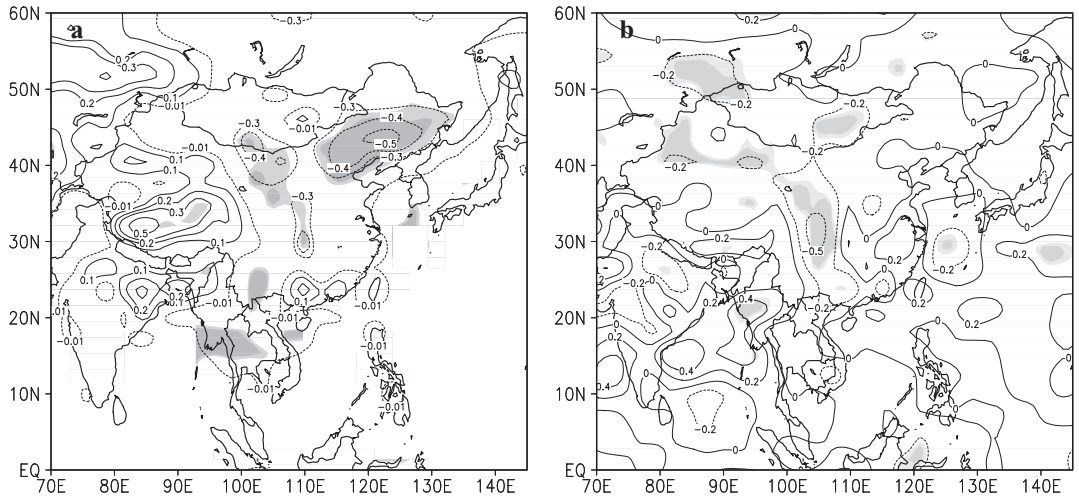

Fig. 9. Changes in: (a) surface temperature (K) and (b) precipitation (mm d^{-1}) induced by BC aerosol in summer over China. Dark and light shades indicate a confidence level of 95 and 90%, respectively, from the *T*-test.

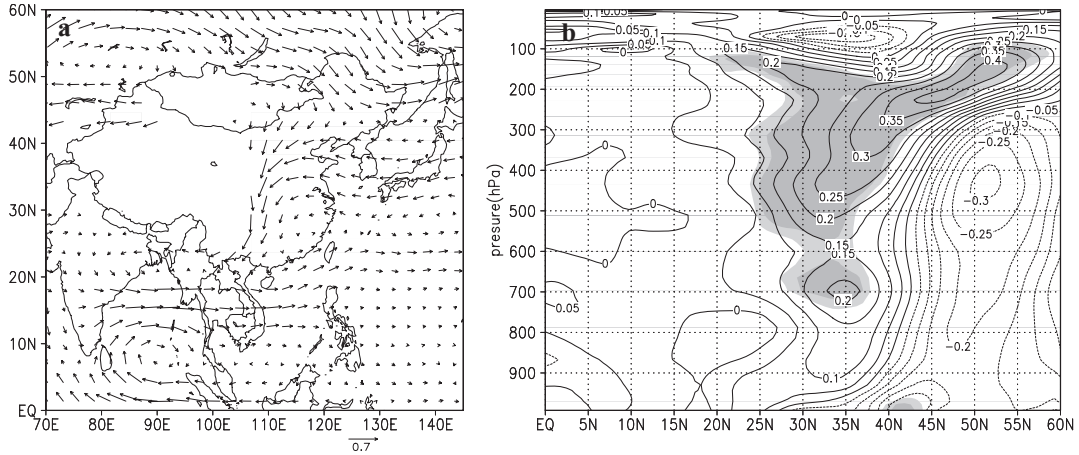

Fig. 10. Changes in: (a) horizontal wind (m s^{-1}) at 850 hPa and (b) vertical temperature (K) zonally averaged between 105°E and 120°E induced by BC aerosol in summer over China. Dark and light shades indicate a confidence level of 95 and 90%, respectively, from the *T*-test.

East China dwindles noticeably and southwesterly wind at the middle latitudes also weakens when it exits from China along the north edge of the subtropical high. It can be inferred from all of these changes that the subtropical high fades and shifts southeastward. However these changes in wind fields including enhanced upward vertical circulation (figures not shown) are statistically insignificant.

We averaged the BC-induced changes of temperature along the latitudes between 105°E and 120°E and are shown in Fig. 10b. Because of the positive radiative forcing from BC aerosols, temperature rises within a very large vertical extent between 20°N and 40°N. To the north of 40°N, however, temperature drops with a significant amount in the middle and upper troposphere. If BC-induced cooling is compared to that induced by sulphate, the area covered by the former is smaller in both vertical and longitudinal directions.

To quantify the cooling effects for BC aerosols, our calculations indicate that monsoon intensity index is reduced by 2.85% for southwesterly wind and by 6.18% for southeasterly wind. Both reductions are smaller than their corresponding values for sulphate aerosols. This result is expected since the cooling effect of BC aerosols is not as strong as that of sulphate aerosols in North China.

To summarize the above results, BC effects on East Asia summer monsoon appear to be more complicated than sulphate effects. Unlike sulphate aerosols that weaken monsoons from all channels, BC aerosols at least strengths southwest monsoon from the second channel and thus causes a smaller reduction in monsoon intensity index than the sulphate aerosols. Considering the different effects on monsoons from these two types of aerosols, it is necessary to study their effects jointly (i.e. 'synthetic aerosols'). We brief our results in Section 4.3.

4.3. Synthetic aerosol

In this section, we describe our results from the sensitivity experiment 'China0'. The global distribution of averaged temperature changes from the last 40 yr (simulation time) very much resembles that from experiment 'sulphate0'. The effects of synthetic aerosols are mainly reflected by the cooling in the Northern Hemisphere. On a global average, surface temperature drops by 0.03 °C, surface pressure increases by 0.3 Pa and precipitation declines by 0.17 mm d^{-1}.

In regard to changes of both horizontal and vertical circulations, we find synthetic aerosols have a similar effect to sulphate aerosols, that is, generally weakening East Asia summer monsoon. Synthetic aerosols cause monsoon intensity index to reduce by 5.15% for southwest monsoon and by 10.04% for southeast monsoon. In addition, similarities are also observed in the global distributions of induced-changes of temperature and precipitation between experiments 'China0' and 'sulphate0'. Just like sulphate and BC aerosols, the effects of synthetic aerosols on monsoons are to cool the earth surface by imposing negative radiative forcing, reduce the thermal and pressure gradients between land and oceans and ultimately weaken the monsoons.

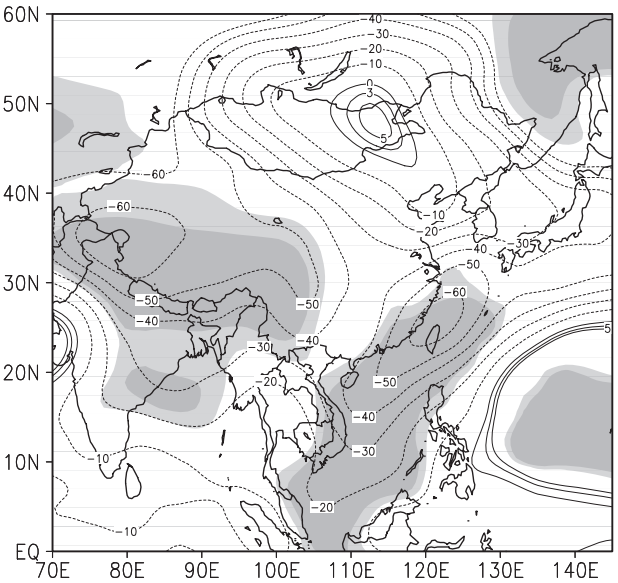

Fig. 12. Changes of surface pressure (Pa) in winter induced by sulphate aerosol. Dark and light shades indicate a confidence level of 95 and 90%, respectively, from the *T*-test.

5. Aerosols' effects on winter (DJF) monsoon

5.1. Sulphate aerosol

With a scattering property, sulphate aerosols reduce the amount of solar energy reaching the earth surface. This is again seen in the sulphate-induced changes of winter surface temperature in China (Fig. 11). Over the landmass of China surface temperature generally declines with a greatest cooling rate of 1.2 °C in South China. Meanwhile, sulphate aerosols induce a warming trend over the oceans to the southeast of China. Surface pressure also changes accordingly (Fig. 12). The maximal surface pressure drop, about 60 hPa, emerges along the coast areas of southeast China and also in the west parts of Tibetan Plateau and Xinjiang Province. Another area with a significant drop of surface pressure (less than 40 hPa) is located in Northeast China. We believe that the generally decreasing trend of surface pressure is a result of warming trend in the middle and upper troposphere induced by sulphate aerosols in winter, despite of their cooling effects at the earth surface. This is supported by Fig. 16, in which the regions with negative changes of surface pressure coincide with those showing a warming trend in the vertical extent of atmosphere.

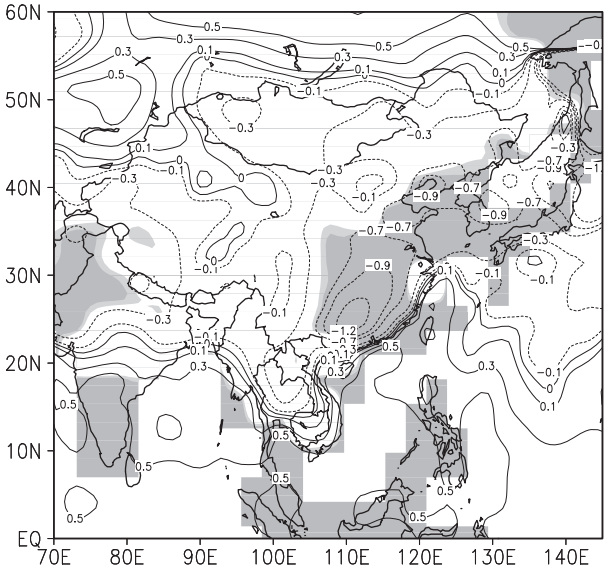

Fig. 11. Changes of surface temperature (K) in winter induced by sulphate aerosol. Dark and light shades indicate a confidence level of 95 and 90%, respectively, from the *T*-test.

East Asia winter monsoon is a typical and distinguished feature on winter 850 hPa weather map. Under current climate conditions, westerly and northwesterly wind prevails to the north of 27°N in China and blows from land to Bohai and East Sea. To the south of 27°N, however, wind direction is reversed so that easterly and northeasterly wind blows from West Pacific to the land. Sulphate-induced changes in wind fields at 850 hPa are exhibited in Fig. 13. One of the main changes is the substantial decline of northeast monsoon in southeast China and its coast areas. To the north of 27°N in East China, the latitudinal component of northwest monsoon weakens greatly while no significant change is observed in its longitudinal component. Northerly wind component increases to the north of 42°N in Northeast China.

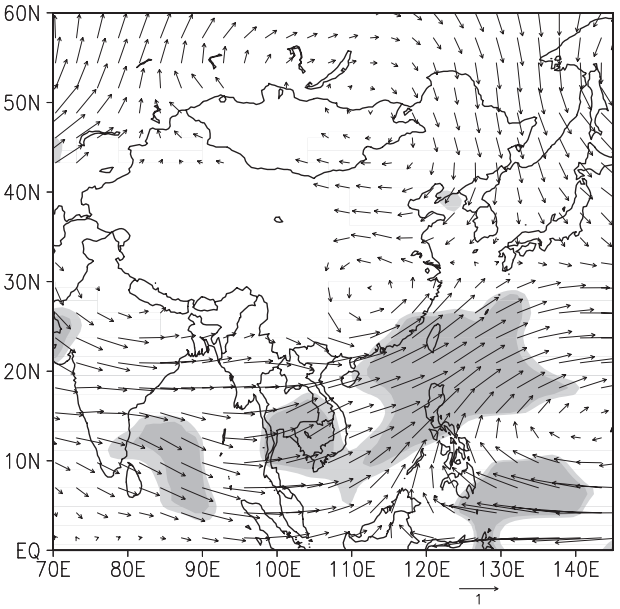

Fig. 13. Changes in horizontal wind (m s^{-1}) at 850 hPa in winter induced by sulphate aerosol in China. Dark and light shades indicate a confidence level of 95 and 90%, respectively, from the *T*-test.

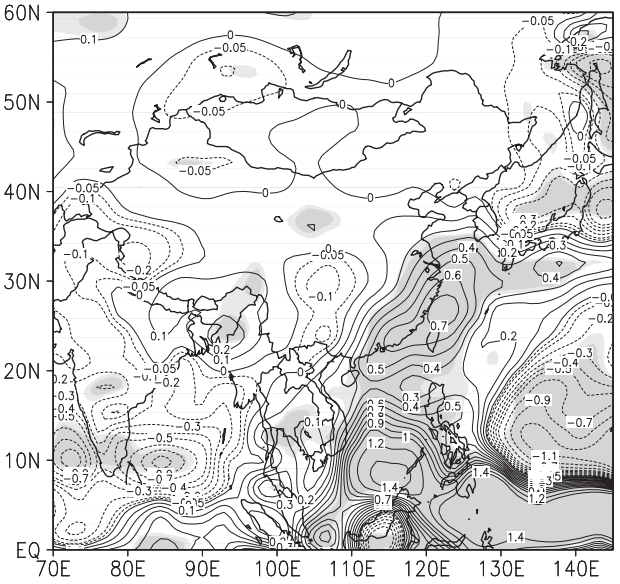

Fig. 14. Changes in precipitation (mm d^{-1}) in winter induced by sulphate aerosol in China. Dark and light shades indicate a confidence level of 95 and 90%, respectively, from the *T*-test.

Akin to other variables, sulphate effects on precipitation are also two-sided (Fig. 14). Winter precipitation very likely decreases in most areas to the north of 40°N, the southwest part of Tibetan Plateau and southwest China, while it could increases in the rest parts of China with the most noticeable increase along the coast areas of East China. In Fig. 15, we partition the sulphate-induced changes of total precipitation into that of convective precipitation and of large-scale precipitation. It is shown that the maximal increase of large-scale precipitation can exceeds 0.4 mm d^{-1} (Fig. 15b). In addition, a comparison between Figs. 14 and 15b indicates a resemblance between changes of total precipitation and of large-scale precipitation. However, this is not the case for the sulphate-induced changes of convective precipitation. These evidences suggest that, on one hand, sulphate effects in winter are mainly to drive the changes of large-scale precipitation and, on the other hand, they are not negligible in affecting convective precipitation because the increasing amount of convective precipitation can be as high as 0.3 mm d^{-1} along the coast areas in southeast China. These findings are different from sulphate effects on summer precipitation.

Under normal conditions in winter, a clockwise meridional circulation evidently exists to the south of 35°N. Within this circulation, the upward motion is located approximately at 10°N and its downward motion is confined between 15°N and 35°N; air flows from south to north in the layers above 500 hPa but reverses its direction below 850 hPa. To the north of 35°N, however, northerly wind prevails and occupies the entire vertical extent of atmosphere. Above 500 hPa and between 35°N and 40°N, air subsides as a result of convergence between northerly wind originated form the north of 35°N and the southerly wind (the poleward component of meridional circulation to the south of 35°N). Below 850 hPa, air uniformly moves southward. Due to the dominance of cold air over warm air, a high-pressure system forms and subsiding motions develop in the region between 30°N and 40°N. Such a wind field represents a typical winter monsoon at its mature phase under normal climate conditions. Figure 16 shows the sulphate-induced changes of meridional circulation and temperature. Again these changes are an averaged result between 105°E and 120°E. A noticeable feature is that sulphate aerosols induce non-uniform temperature changes in the vertical direction. In the areas between 20°N and 50°N, temperature decreases below 850 hPa but increases above this level. The maximal warming takes place between 300 and 200 hPa. When flow field is concerned, sulphate-induced changes are mainly observed to the south of 42°N, such as a weakening trend for northerly winds and subsiding motions. The circulation changes are believed to result in temperature increases in middle and upper troposphere over China.

We quantified the sulphate-induced changes for East Asia winter monsoon by applying monsoon intensity index on its dominant component, northerly wind. Our calculations revealed that the intensity index declined by 2.367%. This suggests that effects of sulphate aerosols in China very likely lead to a weakened East Asia winter monsoon.

5.2. *BC aerosol*

BC-induced changes of surface temperature and total precipitation are shown in Fig. 17. Temperature decreases in a large

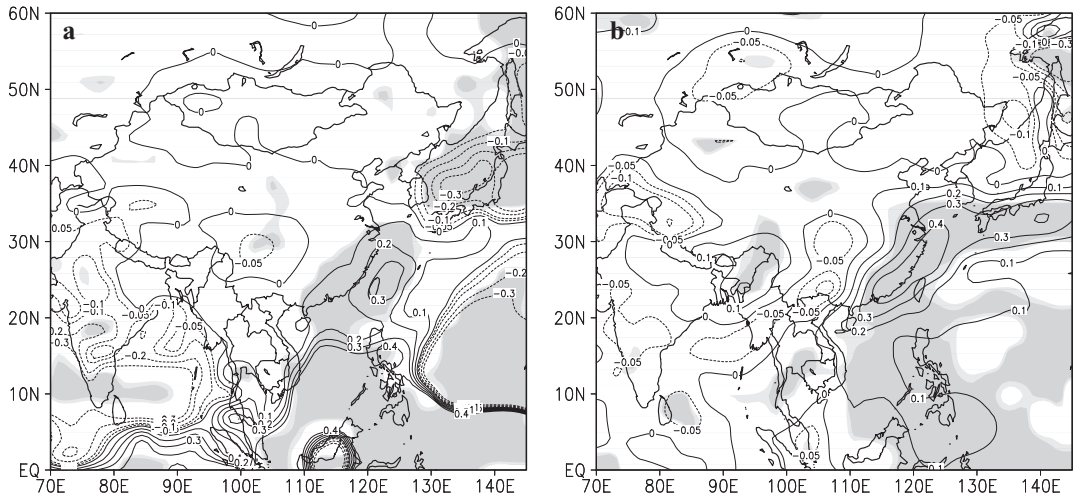

Fig. 15. Change in precipitation (mm d^{-1}) in winter: (a) convective precipitation and (b) large scale precipitation induced by sulphate aerosol. Dark and light shades indicate a confidence level of 95 and 90%, respectively, from the *T*-test.

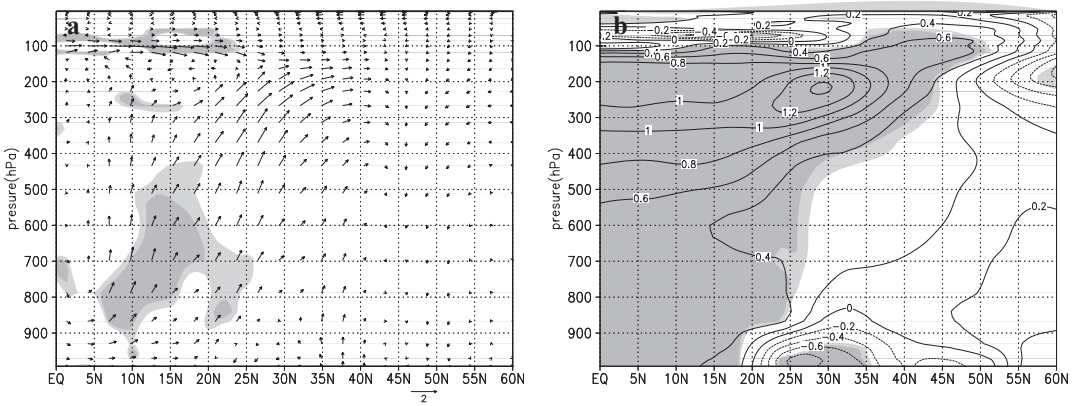

Fig. 16. Changes of: (a) the vertical meridional circulation and (b) temperature (K) zonally averaged between 105°E and 120°E in winter induced by sulphate aerosol. Dark and light shades indicate a confidence level of 95 and 90%, respectively, from the *T*-test.

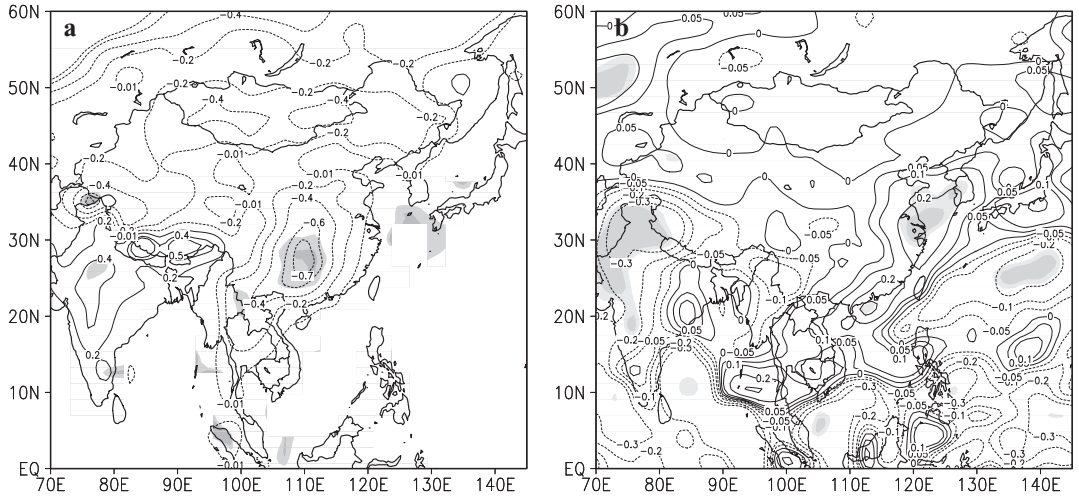

Fig. 17. Changes in: (a) surface temperature (K) and (b) precipitation (mm d^{-1}) induced by BC aerosol in winter over China. Dark and light shades indicate a confidence level of 95 and 90%, respectively, from the *T*-test.

number of areas in China with the greatest cooling trend observed in Central and South China, about −0.6 °C. A warming trend can be seen in some parts of North China and southeast part of Tibetan Plateau. Along the coast areas, temperature changes are overall insignificant. In comparison to sulphate aerosols, BC aerosols apparently cause precipitation to increase in an even broader area that extends further northward and into Northeast China (Fig. 17b). Regardless of their difference in magnitude, both BC and sulphate aerosols exert their influences on total precipitation in a similar manner, that is, by primarily affecting the large-scale precipitation (figure not shown).

BC-induced decreases of surface pressure are also noticeable in most areas other than Northeast China and the east part of Inner Mongolia (figure not shown). Among them the largest pressure decrease, as high as 50 hPa, takes place in East China and the southeast coast areas. Similar to sulphate aerosols, BC aerosols also result in a warming trend within the entire vertical extent of atmosphere (figure not shown), which is a likely cause for the decreased surface pressure in most areas in China.

Figure 18 shows the BC-induced changes of flow field in winter at the level of 850 hPa and temperature profiles averaged in the latitudinal direction between 105°E and 120°E. The main effects of BC aerosols are to weaken East Asia winter monsoon. This is clear in Fig. 18a as the changes of flow field are in an opposite direction to the major wind components of winter monsoon. Little change of wind field is observed in Northeast China. Changes of temperature profiles are also evident (Fig. 18b). BC aerosols induce a temperature decrease close to the ground level and between 20°N and 37°N. Other than that, temperature increases everywhere else with a strongest warming in the layer between 900 and 800 hPa. The BC-induced, zonally averaged (105–120°E) changes of meridional circulation show that all components of winter monsoon appear to dwindle. Among them the subsiding motions at the middle and high latitudes weaken the most. However these changes in meridional circulation fail the *T*-test at 90% confidence level. Once again we quantitatively estimate the BC effects on East Asia winter monsoons and find BC aerosols can reduce the intensity index for northerly wind component by about 3.048%.

5.3. Synthetic aerosol

Considering sulphate and BC aerosols are often released simultaneously from the same sources and co-exist in the atmosphere, it is necessary to study their joint effects on East Asia winter monsoons. Here we analyse their joint effects by treating them as a synthetic aerosol.

In regard to changes of both horizontal and vertical circulations, we find synthetic aerosols have a similar effect to sulphate aerosols, that is, generally weakening East Asia winter monsoon. Synthetic aerosols cause monsoon intensity index to reduce by 5.135%. This value is larger than the decreases of intensity indices resulted from any individual effects of either sulphate or BC aerosols. In other words, the joint effects of these two types of aerosols on temperature and precipitation are much greater than those from either individual, such as: a greatest cooling rate of 1.7 °C in South China and the maximal precipitation increase of 0.9 mm d^{-1} along the coast areas of East China. In addition, just like sulphate aerosol, impacts of synthetic aerosol on total precipitation are also to mainly drive the changes in large-scale precipitation.

6. Discussion and conclusion

In this section, we briefly summarize the results presented above. In summer, effects of sulphate aerosols are predicted to reduce both the thermal and pressure gradient between the landmass of China and the oceans to its east and south. This is because

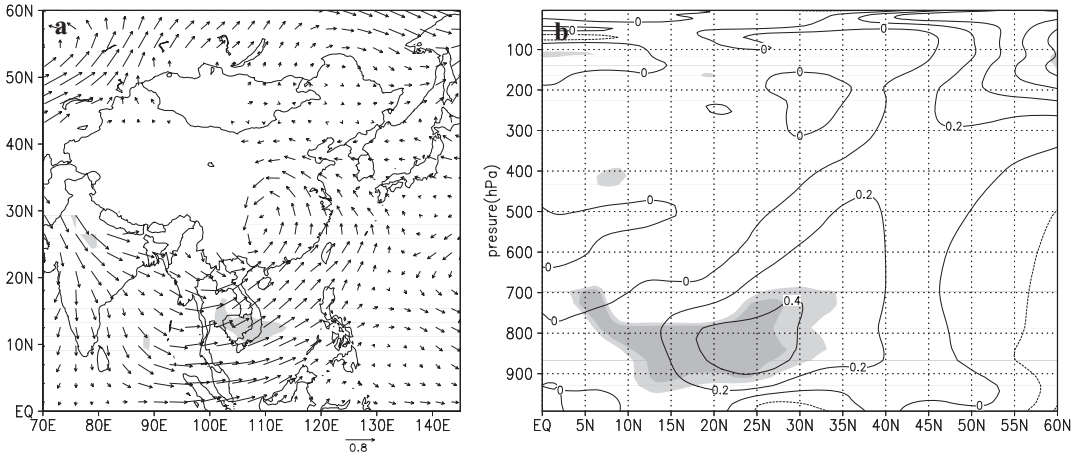

Fig. 18. Changes in (a) horizontal wind (m s^{-1}) at 850 hPa and (b) vertical temperature (K) zonally averaged between 105°E and 120°E induced by BC aerosol in winter over China. Dark and light shades indicate a confidence level of 95 and 90%, respectively, from the *T*-test.

direct radiative forcing by sulphate aerosols leads a cooling trend over the land. Correspondingly, summer monsoons flowing into China from all three channels tend to weaken with the southwest tropical monsoon as the most affected one. In response to the changes in monsoon flow, subtropical high and its accompanied precipitation decline and displace southward into the West Pacific, which ultimately reduces the amount of monsoon precipitation over the land but at the same time increases it over the oceans. A likely feedback from the contrasting changes in precipitation between land and oceans is to further reduce the temperature gradient between them and weaken the summer monsoons, since more latent heat released from precipitation processes is available to warm up the air over the oceans than over the land. The BC aerosols on China region mainly result in changes of temperature and precipitation in Sichuan Basin, and temperature changes in Northeast China, as well as in middle and upper troposphere. Effects of the BC aerosols are relatively small and limited because of their low concentrations.

Synthetic aerosols influence East Asia summer monsoons in a similar manner as sulphate aerosols. For example, the spatial distributions of precipitation changes induced by the former are very much comparable to that caused by the latter. Synthetic aerosols also weaken summer monsoons and alter circulations by radiatively cooling earth surface and thus reducing the temperature and pressure gradients between the land and oceans. As mentioned early, latent heat release in precipitation processes is another important factor in interpreting synthetic aerosols' effects on summer monsoons. As demonstrated in this study, inconsistencies exist between BC and sulphate aerosols on their effects on summer monsoons and hence their joint effects are much more complicated than that of any individual. We therefore, suggest that future studies as such should involve both BC and sulphate aerosols concurrently.

Sulphate and BC aerosols have as important effects on East Asia winter monsoons as on summer monsoons. Sulphate aerosols induce an overall decline of surface temperature in China. Meanwhile, surface pressure declines correspondingly in most areas and over southeastern oceans because of temperature increase in middle and upper troposphere in winter. Adjustments in surface temperature and pressure fields result in a weaken wind field above 850 hPa. A remarkable decrease in northeast monsoon is observed in southeast China and its coast areas. Our estimates of monsoon intensity index reveal that the overall effects from sulphate aerosols are to weaken the winter monsoons in China. Winter precipitation is induced by sulphate aerosols to increases along the coast areas of East China. The changes in winter precipitation are primarily driven by large-scale precipitation except in the coast areas of East China where convective precipitation and large-scale precipitation both contribute.

In winter, BC aerosols affect East Asia winter monsoons in a similar manner as sulphate aerosols. BC aerosols weaken East Asia winter monsoons to a smaller degree than do sulphate aerosols. BC aerosols mainly bring about changes to temperature in Sichuan Basin and low troposphere, as well as precipitation in East China. All of these changes are statistically significant. Although BC concentrations in winter are obviously higher than that in summer, effects of BC aerosols in winter are not significantly stronger than that in summer. It suggests a season-dependence of aerosols' direct effects on climate.

Synthetic aerosols influence East Asia winter monsoons in a similar manner as sulphate aerosols do. For example, the spatial distributions of precipitation changes induced by the former are very much comparable to that caused by the latter. In general, synthetic aerosols not only weaken East Asia winter monsoons to a greater degree than do the individuals, but also result in larger temperature and precipitation changes.

It is demonstrated from our results that the scattering property of sulphate aerosols is well reflected in the changes of East Asia monsoons. In summer, the climatic changes induced by sulphate aerosols mainly include a cooling trend, a weakened summer monsoon, a suppressed convective motion and a decline in precipitation in most areas of China. In winter sulphate aerosols also have an effect in weakening winter monsoon. However, its cooling effect is limited to the low troposphere and temperature increases instead in the middle and upper troposphere, which may results from circulation changes. In regard to winter precipitation, sulphate aerosols lead to a wetting trend in some parts of China, such as the coast areas in southeast and the adjacent waters, and large-scale precipitation is a dominant contributor over convective precipitation. As presented above, our results on BC aerosols clearly reflected their absorbing property. *T*-tests indicate that direct climate effects from BC aerosols over China are relatively weak and limited.

Although both sulphate and BC aerosols generally weaken monsoons in both summer and winter seasons, they certainly differ from each other in affecting vertical structures of temperature and thus atmospheric circulations. Even for a single type of aerosol, its effects on temperature structures and atmospheric circulations are largely season-dependent. It is also evident in our results that the effects of synthetic aerosols on monsoons are not simply a linear summation between BC and sulphate aerosols. Instead, they are determined by their integrated optical properties, such as absorbing versus scattering. As shown in present study, synthetic aerosols to a large degree resemble sulphate aerosols in effecting both summer and winter monsoons. However, the climatic changes induced by the former are in a greater magnitude than the latter, which implies a likely scattering property for the integration of BC and sulphate aerosols. This conclusion can be reasserted if the scattering property of OC aerosols is also taken into consideration. Obviously our findings disagree with Menon et al. (2002). We believe that a key issue in future studies is to determine the integrated optical properties for a mixture of multiple aerosols. Therefore, BC aerosol concentrations and their fraction in total aerosol are the key factors of aerosol climate effects.

7. Acknowledgments

This research was supported by National Basic Research Program of China 973 (Contract number: 2006CB403707 and 2006CB403705).

Dr. Bai Yang's research was supported by U.S. Department of Energy, Office of Science, Biological and Environmental Research (BER), and conducted at Oak Ridge National Laboratory (ORNL), managed by UT-Battelle, LLC, for the U.S. Department of Energy under contract DE-AC05-00OR22725.

Reference

Barth, M. C., Rasch, P. J., Kiehl, J. T., Benkovitz, C. M. and Schwartz, S. E. 2000. Sulphur chemistry in the National Center for Atmospheric Research Community Climate Model: description, evaluation, features and sensitivity to aqueous chemistry. *J. Geophys. Res.* **105**, 1387–1415.

Blanchard, D. C. and Woodcock, A. H. 1980. Production, concentration, and vertical distribution of the sea salt aerosol. *Ann. N. Y. Acad. Sci.* **338**, 330–347.

Bolin, B. and Charlson, R. J. 1976. On the role of the tropospheric sulfur cycle in the short wave radiative climate of the earth. *Ambio*. **5**, 47–54.

Bueh, C. and Ji, L.-R. 1999. Anomaly of East Asia winter monsoon and SST. *Chin. Sci. Bull.* **44**, 252–259.

Chang, C.-P. and Lau, K.-M. 1982. Short-term planetary scale interaction over the tropic and mid-latitudes during northern winter. Part I : contrasts between active and inactive periods. *Mon. Wea. Rev.* **110**, 933–946.

Chen, L.-X., Zhu, Q.-G., Luo, H.-B., He, J.-H., Dongf, M. and co-author. 1991. *East Asia Monsoon*. Chinese Meteorological Press, Beijing, 362 pp.

Chen, L.-X., Zhou, X.-J., Li, W.-L., Luo, Y.-F. and Zhu, W.-Q. 2004. Characteristics of the climate change and its formation mechanism in China in last 80 years. *Acta Meteorol. Sin.*, **62**, 634–645.

Collins, W. D., Rasch, P. J., Eaton, B. E., Khattatov, B., Lamarque, J.-F. and co-author. 2001. Simulating aerosols using a chemical transport model with assimilation of satellite aerosol retrievals: methodology for INDOEX. *J. Geophys. Res.* **106**, 7313–7336.

Collins, W. D., Rasch, P. J., Eaton, B. E., Fillmore, D. W., Kiehl, J. T. and co-authors. 2002. Simulation of aerosol distributions and radiative forcing for INDOEX: regional climate impacts. *J. Geophys. Res.* **107**(D19), 8028, doi:10.1029/2000JD000032.

Collins, W. D., Rasch, P. J., Boville, B. A., Hack, J. J., McCaa, J. R. and co-authors. 2004. Description of the NCAR Community Atmosphere Model (CAM 3.0). NCAR Tech. Note NCAR TN-464+STR, xii+214 pp.

Cooke, W. F., Liousse, C., Cachier, H. and Feichter, J. 1999. Construction of a 1 degrees x 1 degrees fossil fuel emission data set for carbonaceous aerosol and implementation and radiative impact in the ECHAM4 model. *J. Geophys. Res.* **104**, 22137–22162.

IPCC. 2007. Changes in atmospheric constituents and in radiative forcing. In: *Climate Change 2007: The Physical Science Basis. Contribution of Working Group I to the Fourth Assessment Report of the Intergovernmental Panel on Climate Change* [Solomon, S., et al. (eds.)]. Cambridge University Press, Cambridge, United Kingdom and New York, NY, USA, 996 pp.

Gong, W. and Li, W.-L. 1996. Develop of Chinese regional climate model and its preliminary results. In: *Climate Change Mechanism and Numerical Simulation* 2nd Edition (group of 85–913 Program). Chinese Meteorological Press, Beijing, 273–288.

Gu, Y., Liou, K. N., Xue, Y., Mechoso, C. R., Li, W. and co-authors. 2006. Climatic effects of different aerosol types in China simulated by the University of California, Los Angeles atmospheric general circulation model. *J. Geophys. Res.* **111**, D15201, doi:10.1029/2005JD006312.

Hansen, J. E., Sato, M. and Ruedy, R. 1997. Radiative forcing and climate response. *J. Geophys. Res.* **102**(D6), 6831–6864.

Jacobson, M. Z. 2001. Strong radiative heating due to the mixing state of black carbon in atmospheric aerosols. *Nature* **409**, 695–697.

Jacobson, M. Z. and Kaufman, Y. J. 2006. Wind reduction by aerosol particles. *Geophys. Res. Lett.* **33**, L24814, doi:10.1029/2006GL027838.

Lau, K. M. and Boyle, J. S. 1987. Tropical and extra tropical forcing of the large-scale circulation: a diagnostic study. *Mon. Wea. Rev.*, **115**, 400–428.

Lau, K.-M. and Kim, K.-M. 2006. Observational relationships between aerosol and Asian monsoon rainfall and circulation. *Geophys. Res. Lett.*, **33**, L21810, doi:10.1029/2006GL027546.

Lau, K.-M., Kim, M.-K. and Kim, K.-M. 2006. Asian monsoon anomalies induced by aerosol direct effects. *Clim. Dyn.*, **26**, 855–864, doi:10.1007/s00382-006-0114-z.

Liousse, C., Penner, J. E., Chuang, C., Walton, J. J., Eddleman, H. and co-authors. 1996. A global three-dimensional model study of carbonaceous aerosols. *J. Geophys. Res.* **101**, 19 411–19 432.

Luo, Y.-F., Zhou, X.-J. and Li, W.-L. 1999. A numerical study of the atmospheric aerosol climate forcing in China. *Chin. J. Atmos. Sci.* **23**, 1–12.

Luo, Y.-F., Li, W., Lü, D.-R., Li, W.-L. and Zhou, X.-J. 2000. The characteristics of atmospheric aerosol optical depth over China in last 30 years. *Chin. Sci. Bull.* **45**, 549–554.

Luo, Y.-F., Li, W.-L. and Zhou, X.-J. 2001. Analysis of the 1980's atmospheric aerosol optical depth over China. *Acta Meteorol. Sin.* **59**, 77–87.

Mahowald, N., Luo, C., DelCorral, J. and Zender, C. 2003. Interannual variability in atmospheric mineral aerosols from a 22-year model simulation and observational data. *J. Geophys. Res.* **108**(D12), 4352, doi:10.1029/2002JD002821.

Menon, S., Hansen, J., Nazarenko, L. and Luo, Y. 2002. Climate effects of black carbon aerosols in China and India. *Science* **297**, 2250–2253.

Pei, S.-Q. and Li, C.-Y. 2007. A further study on the East Asian winter monsoon and its influences. Part I: features of variation and anomaly. *Clim. Environ. Res.* **12**, 124–136.

Qiao, Y.-T., Chen, L. T. and Zhang, Q.-Y. 2002. The definition of East Asia monsoon indices and their relationship to climate in China. *Chin. J. Atmos. Sci.* **26**, 69–82.

Ramanathan, V., Crutzen, P. J., Kiehl, J. T. and Rosenfeld, D. 2001. Aerosols, climate and the hydrological cycles. *Science* **294**, 2119–2124.

Rasch, P. J., Mahowald, N. M. and Eaton, B. E. 1997. Representations of transport, convection, and the hydrologic cycle in chemical transport models: implications for the modeling of short-lived and soluble species. *J. Geophys. Res.* **102**, 28 127–28 138.

Rasch, P. J., Barth, M. C., Kiehl, J. T., Schwartz, S. E. and Benkovitz, C. M. 2000. A description of the global sulfur cycle and its controlling

processes in the National Center for Atmospheric Research Community Climate Model, Version 3. *J. Geophys. Res.* **105**, 1367–1385.

Singh, R. P., Tare, V. and Tripathi, S. N. 2005. Aerosols, clouds and monsoon. *Curr. Sci.* **88**(9), 1366–1368.

Smith, S. J., Pitcher, H. and Wigley, T. M. L. 2001. Global and regional anthropogenic sulfur dioxide emissions. *Glob. Biogeochem. Cycles* **29**, 99–119.

Stowe, L. L., Ignatov, A. M. and Singh, R. R. 1997. Development, validation, and potential enhancements to the second-generation operational aerosol product at the National Environmental Satellite, Data, and Information Service of the National Oceanic and Atmospheric Administration. *J. Geophys. Res.* **102**, 16 889–16 910.

Tian, H., Ma, J.-Z., Li, W.-L. and Liu, H.-L. 2005. Simulation of forcing of sulfate aerosol on direct radiation and its climate effect over Middle and Eastern China. *J. Appl. Meteorol.* **16**, 322–333.

Zender, C. S., Bian, H. and Newman, D. 2003. Mineral Dust Entrainment And Deposition (DEAD) model: description and 1990's dust climatology. *J. Geophys. Res.* **108**(D14), 4416, doi:10.1029/2002JD002775.